PAPER • **OPEN ACCESS**

The synthesis and study of the electrical properties of composites ($FeAl_2O_3$) with paraffin wax and the determination of the mechanism of electrical conductivity

To cite this article: Ahmed J H Almaliky *et al* 2020 *IOP Conf. Ser.: Mater. Sci. Eng.* **987** 012023

IOP Conf. Series: Materials Science and Engineering **987** (2020) 012023 doi:10.1088/1757-899X/987/1/012023

The synthesis and study of the electrical properties of composites ($FeAl_2O_3$) with paraffin wax and the determination of the mechanism of electrical conductivity

Ahmed J H Almaliky[1], Hussein F Hussein[1] and Khalid I Ajeel[1]

[1]Department of Physics, College of Education for Pure Science, University of Basra, Iraq.

Corresponding author: ahmed.jasem@mail.ru

Abstract. Thick films of composites of iron–aluminium oxide ($FeAl_2O_3$) were prepared by mixing paraffin wax with a powder of aluminium oxide (Al_2O_3) and iron granular (Fe) (600 μm in size). The current–voltage (I-V) characteristic was measured at different temperatures (293–328 K). The electrical conductivity was also measured at those temperature levels. It was noted that an increase in temperature leads to an increase in electrical conductivity. The activation energies (Ea) were determined to be 0.357–0.125 ev; the electrical conductivity mechanism was identified as the Schottky and Poole–Frenkel effects.

1. Introduction

Composite materials have great potential for many technological and industrial applications due to their unique properties, such as low density, ability to form intricate shapes, versatile electrical applications and low manufacturing cost, as well as having a very high dielectric strength, good change storage capacity and dopant-dependent electrical and optical properties. The already wide range of composite applications can be extended by using different materials with inorganic fillers, because dispersed fillers may enhance different physical properties of the host material. The electrical applications of composite solids can be controllably modified depending on many factors, such as the type of the filler used, its concentration, the conductivity of the filler and the method in which it penetrates and interacts with the chains of the polymer [1,2]. To achieve both electrically insulating and thermally conducting polymer composites, alumina is used. Metallic fillers such as graphite and carbon black are used to enhance electrical and thermal properties [3,4]. A nanoparticle is the most basic component in the fabrication of a nanostructure. Metallic nanoparticles have different physical and chemical properties from bulk metals (lower melting points, higher specific surface areas, electronic and optical characteristics, mechanical strength and magnetisation properties that could be used in various industrial applications). Nonconductive fillers increase dielectric permittivity due to interfacial polarisation. The effectiveness of composites depends on their ability to disperse the fillers homogeneously throughout the material [5]. In recent years, studies on the optical and electrical characteristics of composite materials have been the subject of considerable research efforts due to their wide applications in optoelectronic devices. Thin films of the composite $FeAl_2O_3$ with the nano dimension have been studied intensively [6,7]. The physical properties and determination of carrier concentration as well as the mobility of Sb2(Te1-xSex)3 thin films have been investigated [8,9]. The dielectric properties of manganese phthalocyanine (MnPc) thin films have been studied [10]. The influence of sodium zirconate nanoparticles on the structural and

electrical characteristics of polyvinyl alcohol (PVA) nanocomposite films have also been studied [11]. Optical properties of pure and iron-doped cellulose acetate (CA) or PVA have been studied in the 200–800 um wavelength region [12]. The effect of cobalt(II) chloride on the electrical properties of poly(o-toluidine) have been investigated [13]. The synthesis, characteristics and optical properties of polyaniline (PANI) filled by graphene nano-films have also been investigated [14,15].
In the present study, we report on the synthesis and electrical characterisation of $FeAl_2O_3$/paraffin wax composite film of aluminium oxide (Al_2O_3 = 0.07 gm) and iron (Fe = 0.01 and 0.03 gm). The I-V characteristic was measured at different temperatures (283–328 K). Electrical conductivity was also measured at those temperature levels. The activation energies (Ea) and the voltage barrier (ϕ) were determined, and the electrical conductivity mechanism was also studied. At present, a significant scientific concern is the study of the electrical properties of blend and composites [16,17] and also the effect of the insulating matrix material on the electrical and magnetic properties of metal–insulators [18,19,20]. It is considered one of the most successful and sensitive methods in studying the composition of material and also to be important in studying the properties of layer films [21]. The process of determining conduction mechanisms that control the transmission of current through composite materials and physical composites depends on the measurements of the curves (current–voltage and conductivity–temperature) [22]. It may be that there is more than one conduction mechanism in the compound metal–insulator and in the thick film consisting of a specific physical composite, as it depends on the amount of thickness of the prepared film, the intensity of the projected electric field or the degree of deformation.

Table (1): The weight ratio of composites ($FeAl_2O_3$) and activation energies.

Aluminium oxide (AL_2O_3)	0.07 gm	0.07 gm
Iron (Fe)	0.01 gm	0.03 gm
Activation energy (Ea)	0.125 ev	0.357 ev

2. Experimental procedure

The films' composite $FeAl_2O_3$ was prepared by mixing paraffin wax with a powder of aluminium oxide (Al_2O_3) and iron (Fe). The iron element powder was sifted using a granular sieve with a size of 600 μm, and then 0.07 gm of aluminium oxide was mixed with 0.01 and 0.03 gm of a granular iron element with a size of 600 μm, as shown in Table 1. The mixing process was performed using an evaporating dish and a mixing spatula. After the process of mixing was complete, 0.1 gm of paraffin wax was added, which was melted at a temperature of 328 K, while continuing manual mixing as in the previous method. The aluminium slices (2.5*4 cm^2) were washed with acetone and distilled water and then dried in an oven with a temperature of 323 K for 15 minutes. The composition consisting of paraffin paste and aluminium oxide with iron was deposited on aluminium slices. The slices were left in laboratory conditions for 24 hours. The thickness of the samples was measured, and it was found to be 0.448 mm. The aluminium electrodes were deposited in the form of circles with a radius of 1 mm by using the evaporation apparatus under evacuated pressure (10–5 torr). When the electrode deposition process finished, the samples were placed in a special electrode measuring circuit, which consisted of a chamber containing electrodes made of copper. These electrodes were separated by the electric measuring circuit, which consisted of regulated voltages ranging from 1–30 V, where supplied by PHYWE 2592 power. The current was measured by an electrometer type measuring amplifier D53200 L.H.Co. The sample temperature was measured with a thermocouple placed near the sample.

3. Results and discussion

3.1. Measurement of electrical properties

The method of measuring electrical properties plays an important role in providing an accurate description of the change in current with voltages [22,23]. All data were taken after the current stabilised, in which case the current is independent of time. The current–voltage characteristics were measured at different temperatures (293–323 K) and at different concentrations (Al_2O_3 = 0.07 gm; Fe = 0.01 and 0.03), as shown in the Figures 1 and 2. In the two figures, it can be noted that an increase in temperature leads to an increase in current, where both curves display the same behaviour (the ohmic characteristic) at high temperatures, but Figure 1 differs from that characteristic at low temperatures (20–25 K) because of the difference in Fe metal concentration, which in turn leads to the difference in the mechanism of electrical conductivity. When recording values of current and voltage (corresponding to the current), it is followed by raising the temperature of the sample to a temperature higher than its predecessor, which is left for a period of half an hour to reach a degree of thermal stability, and then the process of re-recording the feature (current–voltage) begins; these measurements were repeated until the highest permissible temperature range was reached. Electrical conductivity was measured as a function of temperature of compound samples ($FeAl_2O_3$) for a range of temperatures (293–323 K). Electrical measurements showed an increase in electrical conductivity as the temperatures increased, and this is a traditional behaviour with regard to electrical conductivity in semiconductor materials when increasing the temperature, which in turn leads to an increase in the mobility of the electric charge carriers. Figures 3 and 4 show the linear dependence of electrical conductivity with increasing temperatures and also the hysterical behaviour of electrical conductivity after cooling the samples from 323 to 293 K, which is probably due to the difference in the mechanism of electrical conductivity and also to a decrease in the kinetic energy of the charge carriers.

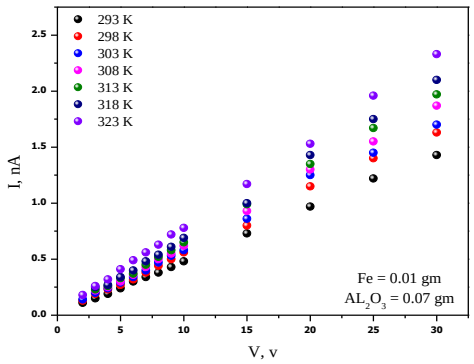

Figure1.The I-V characteristic for sample $FeAl_2O_3$

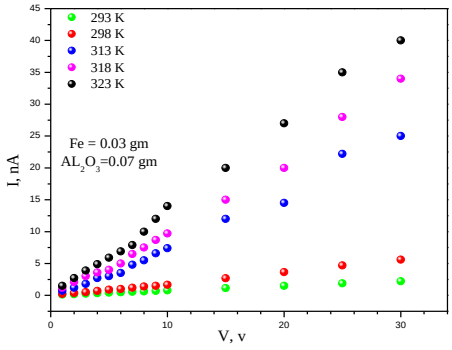

Figure2.The I-V characteristic for sample $FeAl_2O_3$

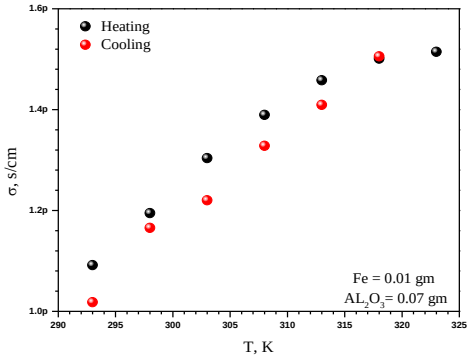

Figure3.Electrical conductivity for sample $FeAL_2O_3$

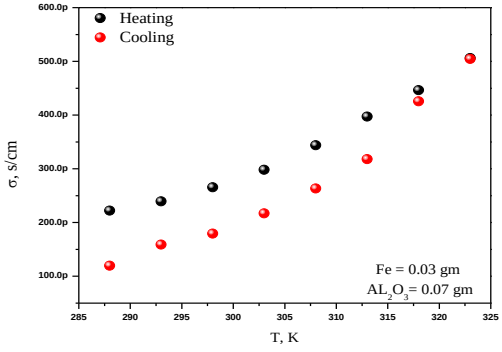

Figure4.Electrical conductivity for sample $FeAL_2O_3$

3.2. Testing conductivity mechanisms for samples $FeAL_2O_3$

3.2.1. Testing the hopping conduction mechanism

The hopping conduction mechanism can be tested by plotting electrical conductivity versus reciprocal temperatures (σ-1000*T-1/4), as shown in Figures 5 and 6, and the plotting of electrical conductivity versus reciprocal temperatures (σ-1000*T-1/3), as shown in Figures 7 and 8, according to the following two equations [24]:

$$\sigma = \exp (Ea/KT1/3) \quad (1)$$

$$\sigma = \exp (Ea/KT1/4) \quad (2)$$

With:
Ea = activation energy (ev)
K = Boltzmann constant (ev/k)
T = temperature (K)
In Figures 5–8, it can be noted that the relationship of conductivity with temperature is non-linear, which indicates the exclusion of this type of conductivity mechanism.

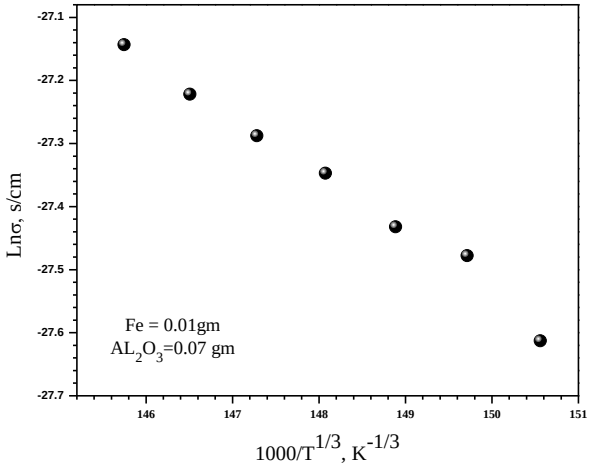

Figure5. The relationship of conductivity with the inverted temperature for composite $FeAL_2O_3$.

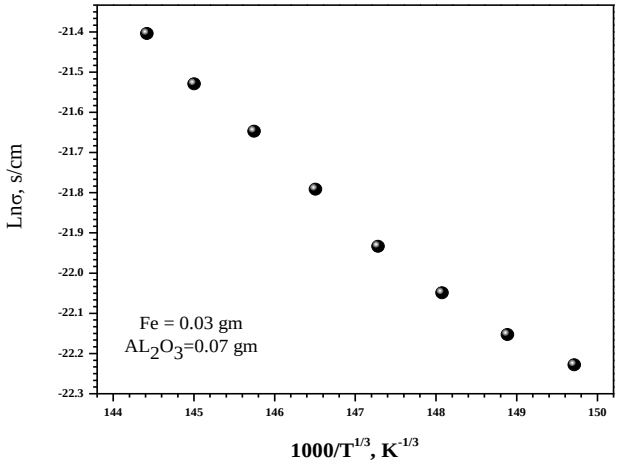

Figure6. The relationship of conductivity with the inverted temperature for composite $FeAL_2O_3$.

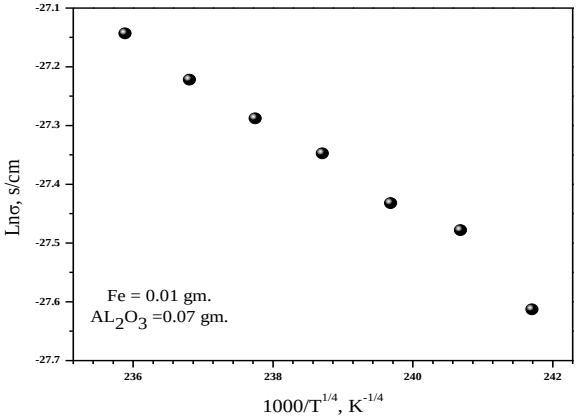

Figure7. The relationship of conductivity with the inverted temperature for composite $FeAL_2O_3$.

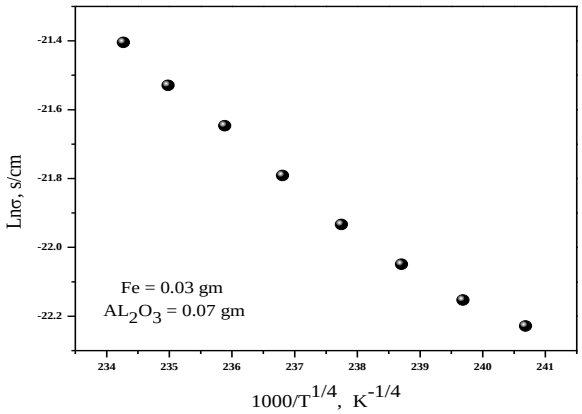

Figure8. The relationship of conductivity with the inverted temperature for composite $FeAL_2O_3$.

3.2.2 Testing the Schottky and Poole–Frenkel conduction mechanisms

Schottky emission [25] is one of the causes of non-ohmic behaviour of the current and occurs when voltage is applied on the metal–insulator contact area. This happens when the electrons transfer from the metal to the conduction band in the dielectric. This mechanism is related to the thermal emission of electrons. In addition, the applied field causes a decrease in the voltage barrier between the metal–dielectric joint. This barrier is affected by the surface layer and the presence of surface trapping centre. The Poole–Frenkel effect [26], or glow discharge [27], is based on the same concept of reducing the voltage barrier to the Schottky effect. However, in this case, electrons are released from the capture trap levels to the conduction beam in the compound. In other words, the difference between the two cases is that the Schottky effect causes a decrease in the voltage barrier at the surface while the Poole–Frenkel effect causes a reduction in the voltage barrier inside the compound. At high voltages, Schottky's mechanism is related with Poole–Frenkel's mechanism in the linear relationship of the I-V feature. Schottky's constant (α_{sh}) is related with Poole–Frenkel's constant (αPF) in the following relationship [28]:

$$\alpha_{sh}=[\frac{q3}{4\pi\epsilon\epsilon_0}]^{1/2} \quad (3)$$

With:
q = electronic charge (C)
ϵ = dielectric constant
ϵ_0 = dielectric constant in the Space (f/m)

Schottky's constant is related with Poole–Frenkel's constant by the following relationship:

$$\alpha_{P.F} = 2\alpha_{sh} \quad (4)$$

Figures 9 and 10 show the relationship between the current and the square root of the voltage of the both samples (Fe = 0.01 and 0.03; AL_2O_3 = 0.07). It is clear that the relationship is linear at high fields. The experimental values of the constant α_{exp} for the examined films can be obtained from the slopes in Figures 9 and 10 in the straight line in the high field region. The theoretical values of α_{sh} and $\alpha_{P.F}$ can be determined with the help of Equations 3 and 4. The experimental values α_{exp} in Tables 2 and 3 are close to the theoretical value $\alpha_{P.F}$, which indicates that the Poole–Frenkel effect is a dominant mechanism, so the applied filed is enough to enhance the thermal exited electron inside the composite films.

Table2. Experimental and determined α values from Schottky's and Poole–Frenkel's theories and the dielectric constant for composite sample $FeAL_2O_3$, where Fe = 0.01 gm and AL_2O_3 = 0.07 gm.

T (K)	α_{exp}	α_{sh}	$\alpha_{P.F}$	ϵ
293	0.082	0.045	0.09	0.60
298	0.065	0.037	0.07	0.45
313	0.041	0.027	0.05	0.22
318	0.036	0.018	0.036	0.10
323	0.032	0.016	0.033	0.085

Table3. Experimental and determined α values from Schottky's and Poole–Frenkel's theories and the dielectric constant for composite sample $FeAL_2O_3$, where Fe = 0.03 gm and AL_2O_3 = 0.07 gm.

T (K)	α_{exp}	α_{sh}	$\alpha_{P.F}$	ϵ
293	0.03611	0.0461	0.09219	0.169
298	0.03602	0.04592	0.09184	0.109
303	0.03597	0.04583	0.09165	0.076
308	0.03592	0.04576	0.09152	0.056
313	0.03586	0.04569	0.09139	0.043
318	0.03582	0.04561	0.09122	0.034
323	0.03574	0.04530	0.09060	0.028

Figures 11 and 12 represent the relationship between log Io/T2 versus reciprocal temperature (Richardson plot), where Io represents the extrapolation of current (Fe = 0.01 and 0.03; AL_2O_3 = 0.07). The lowering of the work function ($\Delta\phi$) for the thermionic emission due to the Schottky effect can be determined from the following relation [29]:

$$\Delta\phi=[\frac{eE}{4\pi\epsilon\epsilon_0}]^{1/2} \qquad (5)$$

With:
e = the electronic charge (C)
E = electric field ϵ the dielectric constant (v/m)
These are shown in Figures 13 and 14 for both samples Fe = 0.01 and 0.03 and Al_2O_3 = 0.07.

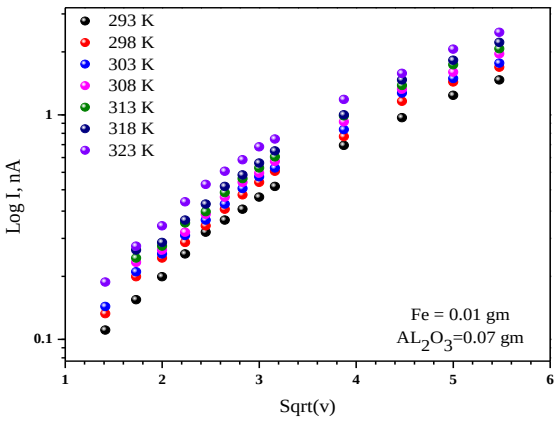

Figure9. Plots of log(I) with square root of V for sample of composite $FeAL_2O_3$ at several temp. (293–323 K).

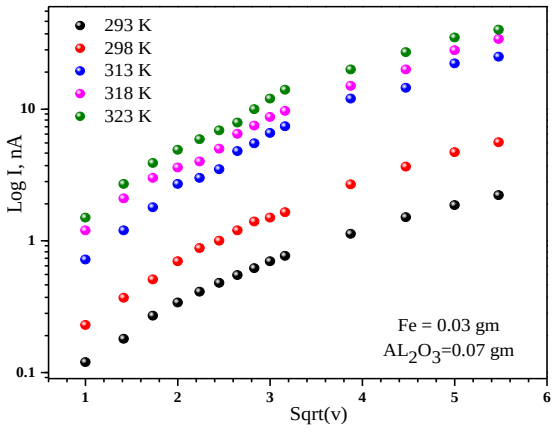

Figure10. Plots of log(I) with square root of V for sample of composite $FeAL_2O_3$ at several temp. (293–323 K).

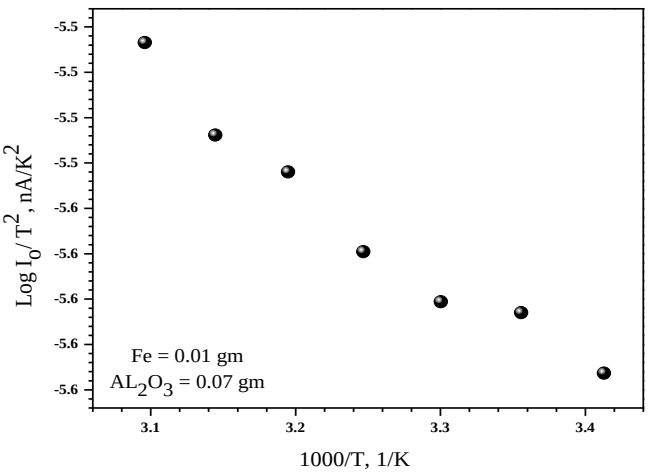

Figure11. Plot of log Io/T2 - 1/T (K-1) for $FeAL_2O_3$ film.

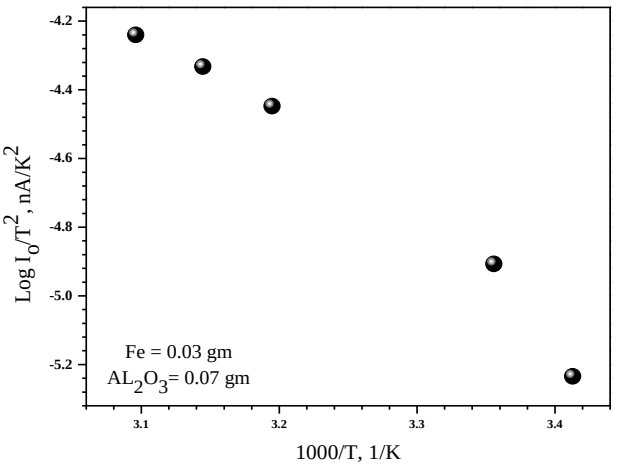

Figure12. Plot of log Io/T2 - 1/T (K-1) for $FeAL_2O_3$ film.

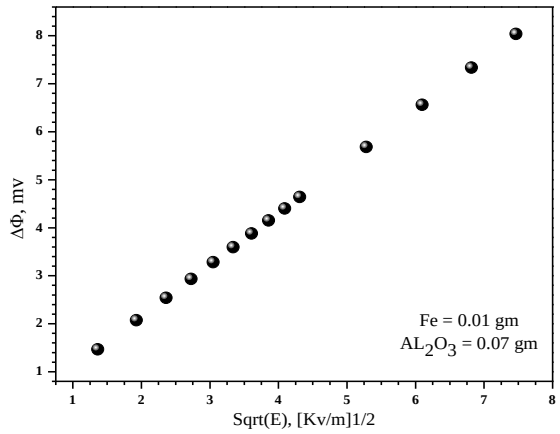

Figure13. The relationship between the lowering potential barrier versus E1/2 for $FeAL_2O_3$ samples at room temperature.

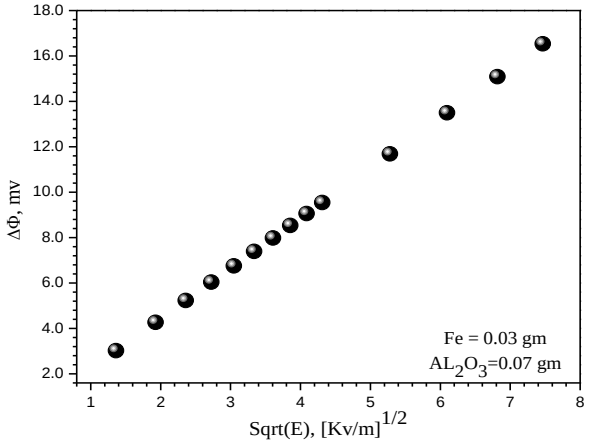

Figure14. The relationship between the lowering potential barrier versus E1/2 for $FeAL_2O_3$ samples at room temperature.

3.3.3 Testing the ion conduction mechanism

The mechanism of ion conduction was tested by drawing the relationship between -L-nσ T1/2 and 1000/T K - 1 according to the following formula [29]:

$$\sigma = \frac{\sigma_0}{\sqrt{T}} \exp\left(-\frac{Ea}{KT}\right) \qquad (6)$$

with:

σ_0 = constant

Figures 15 and 16 show the plots of -L-nσ T1/2 versus 1000/T K - 1, where the ion conduction mechanism can be expected to occur if the data show linear dependence. Furthermore, the current–voltage characteristics do not obey the general ionic equation (hyperbolic sine relationship); the tunnelling mechanism is also not applicable in our study, because it requires very thin films, where the current is independent of temperature, but we have thick films (as shown in Table 4), where the current is dependent on temperature.

Table 4. The thickness and concentrations of both samples.

Composite	Fe	AL_2O_3	Thickness
Fe	0.01 gm	0.07 gm	0.448 mm
AL_2O_3	0.03 gm	0.07 gm	0.538 mm

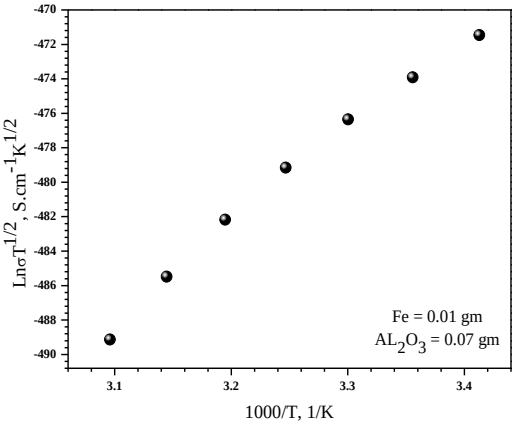

Figure 15.The relationship between Ln ($\sigma T^{1/2}$) versus 1000/T for $FeAL_2O_3$ for the ionic conduction test.

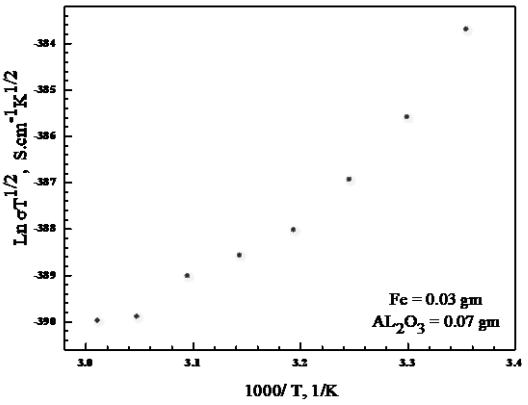

Figure 16.The relationship between Ln ($\sigma T^{1/2}$) versus 1000/T for $FeAL_2O_3$ for the ionic conduction test.

4. Conclusions

The following conclusions can be drawn from this study of the two samples of iron–aluminium oxide composite ($FeAl_2O_3$), where Fe = 0.01 and 0.03 and Al_2O_3 = 0.07. Electrical properties and determination of the mechanism of electrical conductivity have been investigated in the temperature range 293–323 K; the conduction mechanisms were identified by measuring the current–voltage (I-V) characteristics and current–temperature dependence equations. For sample $FeAl_2O_3$ with Fe = 0.01 gm, Schottky's conduction mechanism is dominant, where its electrical characteristics are explained by comparing α constants and by studying the dependence of conductivity with different work functions. However, for sample $FeAl_2O_3$ with Fe = 0.03 gm, Poole–Frenkel's conduction mechanism is dominant. Other mechanisms (i.e. ion conduction mechanism and hopping conduction mechanism) were also investigated, but they were excluded from our expectations. On the other hand, we found some difference between these two samples in their electrical properties in the values of α constants therefore in conduction mechanism, and finally in some electrical factors (σ, Φ and I), because of the different in thickness and the concentration of metal in each sample.

5.References.

[1] Golden J H, Hawker C J and Ho P S 2001 Designing porous low –K Dielectric *semiconductor international* **24** 79-87

[2] Abdullah O G and Saber D R 2012 optical absorption of PVA films doped with Nickel chloride *applied mechanics and materials* **110-116** 117 -182

[3] XU Y, Chung D D L and Mroz C 2001Thermally conducting Alumium Nitride polymer matrix Composites *Composites Part A: Applied science and manufacturing* **32** 1749- 1757

[4] Mamuny Y p, Davydenko V V, Pissis P and Lebedev E V 2002 Electrical and thermal conductivity of polymer s filied with metal powder *European polymer journal* **38** 1887-1897

[5] Pillai P K C, Narula G K and Tripathi A k 1984 Dielectric properties of poly propylene / poly carbonate poly blend *polymer journal* **16**, 575-578

[6] Stognei O V, Al-Maliki A, Sitnikov A and Makagonov V 2015 Thermoelectric Power of Gradient $Fe_x(Al_2O_3)_{100-x}$ Composite Films *Solid State Phenomena* **233-234** 694-698..

[7] Stognei O V ,Sitnikov AV and Al-Maliky A J 2014 PREPARATION OF Fex (Al2On)100-x CONCENTRATION-GRADIENT COMPOSITE FILMS *Bulletin of the Voronezh State Technical University* **10-1** 7-11

[8] Ajeel Khalid I and Khalid Usama A 2003 Synthesis and study the physical properties of $Sb_2(Te_{1-x}Se_x)_3$ compound *Journal of Basrah Researches/Science* **29** 2
[9] Ajeel Khalid I and Khalid Usama A 2003 Investigation of transport phenomina and determination of carrier concentration and mobility of $Sb_2(Te_{1-x}Se_x)_3$ compound *Journal of Basrah Researches/Science* **29** 2
[10] Ajeel Khalid I and Hussein H F 2003 preparation and studying the dielectric properties of manganese metal phthalocynine (MnPC) Thin films *Iraqi J.Polymers* **7 No.1** 75-82
[11] Chandrala H N , Ramaraj B, Shivakumaraiah, Madhu G M and Siddaramuiah 2013 investigation on the influence of sodium zirconate nanoparticles on the structural characteristics and electrical properties of polyvinyl alcohol nanocomposites films *Journal of alloys and compoundes* **555** 531 -538
[12] Sharma Aa k and Rama C H 1991 optical properties of pure and iron doped cellulose acetate *Journal of materials science letters* **10** 1217-1219
[13] Fakher R K and Ajeel K I International journal 2015 Effect of cobalts chloride on Electrical properties of poly (O-Toluidine) *International Journal Of materials science and Engineering* **3** 4
[14] Ajeel Khalid I and Kareem Q S 2019 Synthesis and characteristics of Polyaniline (PANI) Fillid by Graphene (GR) Nano film *IOP. Con. Journal of Physics: Conference Series* 1234.
[15] Ajeel Khalid I and Kareem Q S 2019 Optical properties for prepared Polyaniline (PANI) Fillid by Graphene (GR) Nanocomposites films *Journal of Basrah Researches/Science* **45** 2
[16] Beles B A, Sheng P, M D Abeles, Coutts B and Arie Y 1975 Structural and electrical properties of granular metal films *Advances in Physics* **24** 407-461
[17] Beloborodov I S, Lopatin A V, Vinokur V M, and Efetov K B 2007 Granular Electronic Systems *Rev. Mod. Phys.* **79** 469-518
[18] Dempsey N et.al 2001 agnetic behavior of Fe:Al2O3 nanocomposite films produced by pulsed laser deposition *Journal of Applied Physics* **90 12** 6268-6274
[19] Batlle X, Labarta A 2002 Finite-size effects in fine particles: magnetic and transport properties *Journal of Physics D: Applied Physics* **35** R15-R42
[20] Hutten A, Sudfeld D, Wojczykowski K, Jutzi Peter and Reiss G 2003 Giant magneto resistance and magnetic aspects in granular structures *Journal of Magnetism and Magnetic Materials* **262** 23-31
[21] Hill R M 1969 Electrical Conduction in Ultra-Thin Metal Films *Proceedings of the Royal Society A* **309** 377-395
[22] Ebade S S 2014 Preparation the copolymers and studying its electrical properties and used electronic application *MSc.thesis submitted to college of pure science University of Basrah/Iraq.*
[23] Abdul Ghafor WAS 2000 Schottky Effect Mechanism in Poly (pyromellitic-4,4-diphenyl sulphone) Films *Journal of Polymer Science: Part B: Polymer Physics* **38** 2507–2514
[24] Abdul Ghafor WAS, W Z Manookien and G A Adam 1997 Iraqi polymer journal **1** 59
[25] Deal B E, Fleming P J and Castro P L 1968 Electrical Properties of Vapor-Deposited Silicon Nitride and Silicon Oxide Films on Silicon *Journal of The Electrochemical Society* **115** 3
[26] Lilly A C and McDowell J R 1968 High-Field Conduction in Films of Mylar and Teflon *Journal of Apply Physics* **39** 141
[27] Frenkel 1938 On Pre-Breakdown Phenomena in Insulators and Electronic Semi-ConductorsJournal of Physical review **54** 467
[28] Abdul Ghafor W A S 1996 Synthesis , characterisation and study of some New Condensated polymers, their Electrical properties and Application as FET *Ph.D.* thesis Basrah university/Iraq.
[29] wenkuo C, Huang C Wen, Chen B Kuan, Li W Bin, Chen P Rong, Ho T Han, Tseng C Guey and Wu T Yi 2013 Enhanced Ionic Conductivity in PAN-PEGME-$LiClO_4$-PC Composite polymer Electrolytes *Int.J.Electrochem.Sci* **8** 3834-3850